34th Annual International Conference of the IEEE EMBS
San Diego, California USA, 28 August - 1 September, 2012

Power Line Interference Cancellation in In-vivo Neural Recording

Mohammad Reza Keshtkaran and Zhi Yang

Abstract— **This paper presents an algorithm for removing power line interference in neural recording experiments. It does not require any interference reference signal and can reliably track interference changes in frequency, phase, and amplitude. The method includes three major steps. First, it employs a robust frequency estimator to obtain the fundamental frequency of the interference. Second, a series of discrete-time oscillators are used to generate interference harmonics, where harmonic phase and amplitude are obtained using the recursive least squares (RLS) algorithm. Third, the estimated interference harmonics are removed without distorting the neural signals at the interference frequencies. The simple structure and adequate numerical behavior of the algorithm renders it suitable for real-time implementation. Extensive experiments based on both in-vivo and synthesized data have been performed, where a reliable performance has been observed.**

I. Introduction

Extracellular neural recording using microelectrode arrays can provide high fidelity signals of both single- and multi-unit activities and field potentials. Single- and multi- unit activities are spike trains that have a dominant spectrum in 400-5000 Hz, while local field potentials (LFPs) are aggregated from a large number of synchronized synaptic activities with a dominant spectrum in 0.1-200 Hz. Both spike trains and field potentials are useful for information decoding; however, due to better tolerance to neural interface degeneration and glial cell encapsulation, field potentials have been receiving increasing attention in long-term brain machine interface (BMI) experiments [1].

Recorded field potentials are frequently contaminated with power line interference (also called 50/60 Hz noise), which could be large in magnitude and may severely corrupt the information content of LFP signals. For example, Gamma oscillations (>30 Hz) which are correlated with a wide range of cognitive and sensory processes, may be distorted by the interference. Therefore, adequate removal of interfering components would be an important preprocessing stage to achieve a reliable analysis of LFP signals.

Different solutions such as using battery power, high common-mode rejection ratio (CMRR) amplifiers and Faraday cage, can be used to attenuate the interference and avoid electronic saturation. In addition, various algorithms have been reported to remove power line interference. From application aspects, a robust and real-time algorithm which can eliminate the interference without distorting the LFP signals is desirable. Along this line, Wang and Roe [2] have recently employed an adaptive noise canceller (ANC) to remove the interference in neural recording. The method was first proposed by Widrow for processing ECG signals [3] and works well if given a high quality interference reference signal, which is not always available in experiments.

In this paper, we propose a novel algorithm for power line interference cancellation. The algorithm requires no interference reference signal and it can reliably track interference changes in frequency, phase, and amplitude at 50/60 Hz and the harmonic frequencies. Based on different statistical characteristics of the interference components and LFP oscillations, the algorithm can eliminate the interference without distorting the LFP signals at the interference frequencies. Further efforts have been spent to reduce the computational requirement of the algorithm to target real-time, low-latency ASIC implementation. Extensive experiments based on both in-vivo and synthesized data have been performed, where a reliable performance has been observed.

The rest of the paper is organized as follows. Section II gives the problem overview and the algorithm framework. Section III presents the algorithm details. Section IV describes the experimental results on both in-vivo and synthesized data. Finally, Section V concludes the paper.

II. Problem Overview and Algorithm Framework

A. Problem Overview and Application Related Challenges

Power line interference can be modeled as the sum of harmonic sinusoids with undetermined frequencies, phases and amplitudes. The problem of unsupervised interference cancellation involves the estimation of frequencies, amplitudes and phases of interference sinusoidal components and subsequently removing the estimated interference from the recorded signal. Various methods have been proposed for interference removal from biomedical signals [4], [5], [6]; however, there are a few application related challenges that affect the performance of these methods when applied to neural recording. For example, the spectrum of neural data follows $1/f^{x}{}_{(1<x<3)}$ distribution that violates the assumption of white Gaussian noise made in many algorithms and may cause algorithm malfunction. Moreover, neural signals are non-stationary and there could be transient or sustained LFP oscillations appearing at the interference frequencies that should remain intact. For example, [4] used adaptation blocking in the QRS period of ECG signals to tackle non-stationarity; however, this method is not applicable to neural signals because the on/off period of LFP oscillations cannot be easily detected in the presence of interference. Last, the

This work is supported by Singapore Public Sector Funding R-263-000-699-305, MOE grant R-263-000-619-133 and SERC grant R-263-000-656-305

Mohammad Reza Keshtkaran and Zhi Yang are with the Department of Electrical and Computer Engineering, National University of Singapore, 117576, Singapore (e-mail: {keshtkaran,eleyangz}@nus.edu.sg)

algorithm is preferable to be efficient in hardware implementation, targeting real-time and low-latency preprocessing of neural signals in less constrained environments.

B. Algorithm Framework and Contributions

In this section, a few important features of the algorithm are summarized. First, the algorithm yields a robust and fast estimation of the interference fundamental frequency, which is hardly affected by the colored spectrum of the input signal. Based on the estimated fundamental frequency, the selected interference harmonics are estimated and then removed accordingly. Second, the proposed algorithm allows using different rates for frequency and amplitude adaptation, which result in an accurate frequency estimation while reliably tracking interference amplitude fluctuations. As a result, the algorithm can reliably work in situations where the appeared harmonics may vary in frequency, phase, and amplitude. Third, the proposed algorithm has been tailored for fixed-point operation and can be efficiently implemented in both software and hardware.

III. METHODS

Recorded neural data can be modeled as

$$y(t) = s(t) + p(t) \tag{1}$$

where, $y(t)$ is the recorded signal, $s(t)$ is the actual signal (neural signal and neural noise) and $p(t)$ is the power line interference. $s(t)$ has a $1/f^x$ power spectrum and $p(t)$ consists of a set of harmonic sinusoidal components with unknown frequencies, phases and amplitudes as shown in (2a)

$$p(t) = \sum_{k=1}^{M} a_k \cos(k\omega_f t + \phi_k) = \sum_{k=1}^{M} h_k(t) \tag{2a}$$

with

$$h_k(t) = a_k \cos(k\omega_f t + \phi_k), \tag{2b}$$

where M is the number of harmonic components appearing in $p(t)$, ω_f is the fundamental frequency, and a_k and ϕ_k are the amplitude and phase of the k^{th} harmonic, respectively.

Let $\hat{\omega}_f$, $\hat{a}_k$, $\hat{\phi}_k$, $\hat{h}_k(t)$ and $\hat{p}(t)$ denote the estimate of ω_f, a_k, ϕ_k, $h_k(t)$ and $p(t)$, respectively. Hence, the interference-free signal $\hat{s}(t)$ is obtained by

$$\hat{s}(t) = y(t) - \hat{p}(t). \tag{3}$$

The following approach is proposed to obtain $\hat{p}(t)$. First, fundamental frequency is estimated by using a fast and numerically well-behaved lattice-based frequency estimator. Subsequently, harmonic signals are obtained by using discrete-time oscillators and their amplitudes and phases (i.e. $\hat{a}_k$ and $\hat{\phi}_k$, respectively) are adapted using the recursive least squares (RLS) algorithm [7]. Finally, the estimated interference is subtracted from the signal. The structure of the proposed method is shown in Fig. 1.

A. Fundamental Frequency Estimation

Two stages of processing are used to obtain the fundamental frequency of the interference.

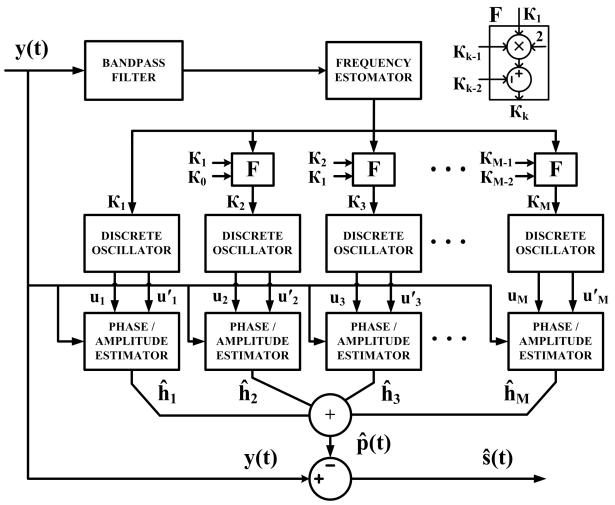

Fig. 1. Block diagram of the proposed structure. $y(t)$ is the contaminated input signal and $\hat{s}(t)$ is the output interference-free signal.

1) Initial Bandpass Filtering: Before feeding the signal to the frequency estimator, a second order infinite-impulse-response (IIR) bandpass filter with passing band of 40-70 Hz is utilized to attenuate unwanted frequency components due to the following two reasons: a.) the spectrum of $s(t)$ and hence $y(t)$ in (1) follows $1/f^x$ distribution that may lead to a biased estimate of the frequency in some frequency estimators. b.) when higher harmonics exist in the interference, direct application of a single frequency estimator may lead to the estimation of higher harmonic frequencies instead of the fundamental frequency.

2) Frequency Estimation: After bandpass filtering, frequency estimation is performed by using a simplified lattice-type adaptive notch filter (ANF) [8] shown in Fig. 2(a). Lattice adaptive filters are known to have fast convergence and attractive numerical and stability properties when compared with direct-form filters that make them more suitable for finite-precision and real-time implementation [8], [9]. The parameters κ_f and α in Fig. 2(a) are reflection coefficients; κ_f is related to notch frequency $\hat{\omega}_f$ by (4) and α controls the notch bandwidth. The value of α should be chosen close to unity to achieve a narrow notch. Frequency estimation is obtained by adapting κ_f in the structure of Fig. 2(a). In this work, Burg algorithm [8] is used to adapt κ_f due to its fast convergence and guaranteed stability. κ_f is defined as

$$\kappa_f = \cos\hat{\omega}_f \tag{4}$$

The algorithm to adapt κ_f in the structure of Fig. 2(a) is:

$$\kappa_f(n) = \frac{C(n)}{D(n)} \tag{5a}$$

$$C(n) = \lambda_f C(n-1) + f_0(n)b_0(n) \tag{5b}$$

$$D(n) = \lambda_f D(n-1) + 0.5(f_0^2(n) + b_0^2(n)) \tag{5c}$$

$$C(0) = D(0) \gg 0, \quad 0 \ll \lambda_f < 1 \tag{5d}$$

where λ_f is the forgetting factor and $\kappa_f(n)$ is the estimated parameter associated with the n^{th} sample. The relationship between $\kappa_f(n)$ and the fundamental frequency is specified

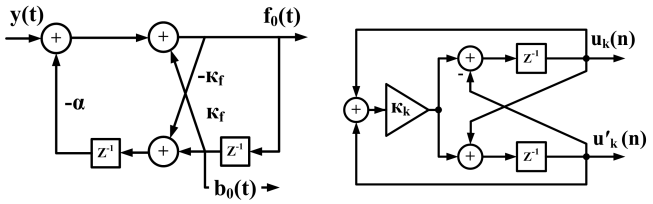

(a) (b)

Fig. 2. Signal flow graph of (a) Lattice frequency estimator and (b) Discrete-time Oscillator.

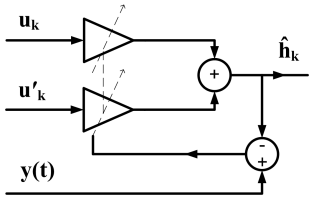

Fig. 3. Adaptive filter structure used for phase and amplitude adaptation. The filter weights are adapted by using RLS algorithm.

by (4). After estimating κ_f, harmonic frequencies can be readily obtained without inverse trigonometric calculations as discussed later.

B. Harmonic Estimation

After estimating κ_f, the algorithm proceeds to the estimation of the harmonics of the interference. In this work, discrete-time oscillators are used for harmonic estimation that is to avoid trigonometric function calculations thus reducing complexity. Furthermore, this technique allows independent control of frequency and amplitude adaptation via using different adaptation rates to achieve accurate frequency estimation while reliably tracking amplitude variations.

Among different types of oscillators, a Digital Waveguide Oscillator [10] is chosen due to the following reasons. First, it provides quadrature outputs which are exploited to simplify the phase and amplitude adaptation algorithm. Second and more importantly, the oscillator output frequency can be directly controlled by $\cos\omega$ where ω is the oscillation frequency. This property is desirable as it allows the frequency estimator output κ_f to be directly used in the discrete oscillators in order to adjust their frequencies. These considerations eliminate the need for trigonometric function calculation hence significantly reducing the complexity of the algorithm. Fig. 2(b) shows the signal flow graph of the oscillator. The parameter κ_k in Fig. 2(b) is defined as

$$\kappa_k = \cos(k\hat{\omega}_f), \quad \text{for } k = 1, 2, \cdots, M \tag{6}$$

where $k\hat{\omega}_f$ is the estimated frequency of the k^{th} harmonic component. The output of each oscillator is of the form

$$u_k(n) = v_k \sin(k\hat{\omega}_f n) \tag{7a}$$

$$u'_k(n) = v'_k \cos(k\hat{\omega}_f n) \tag{7b}$$

where v_k and v'_k are the magnitudes and $k\hat{\omega}_f$ is the oscillation frequency; all pertaining to the k^{th} harmonic. It should be noted that for each k, v_k and v'_k are constant, however, not equal to each other. In order to keep v_ks and v'_ks fixed throughout the oscillation, gain control is applied in each iteration [10].

In order to override trigonometric function calculation for obtaining $\hat{\omega}_f$ and κ_ks, the values of κ_ks in (6) are recursively calculated through Chebyshev method as

$$\kappa_k = 2\kappa_1\kappa_{k-1} - \kappa_{k-2}, \quad \text{for } k = 2, 3, \cdots, M \tag{8a}$$

where

$$\kappa_0 = 1, \kappa_1 = \kappa_f = \cos\hat{\omega}_f \tag{8b}$$

The values of κ_ks are then used to adjust the operation frequency of the oscillators.

C. Phase and Amplitude Estimation

The phases and amplitudes of the generated sinusoids are not necessarily the same with their corresponding interference components; therefore, an additional step is required for phase and amplitude estimation. Since a pair of orthogonal signals (u_ks and u'_ks) are available from the output of each oscillator, the phase and amplitude adaptation can be expressed as a simple linear combination of the orthogonal outputs. For this purpose, an adaptive linear combiner is utilized which is shown in Fig. 3. For each harmonic k, the optimal weights can be obtained by minimizing the exponentially weighted squared error between $\hat{h}_k(t)$ and $y(t)$. This can be done by using the RLS algorithm [7] where $u_k(n)$ and $u'_k(n)$ serve as the inputs of the adaptive linear combiner. The estimated harmonics, denoted by $\hat{h}_k(t)$ in (2b), are then subtracted from $y(t)$ to obtain the interference-free signal $\hat{s}(t)$.

IV. Simulation Results

A. Evaluation on Synthesized Data

For synthesizing contaminated neural recording data, harmonic sinusoidal components with random fundamental frequency around 60 Hz were added to an interference-free signal ("interference-free" signal is referred to the neural signal which was recorded in a controlled condition where power line interference was very small). The frequencies, amplitudes and phases of the components were randomly chosen and then perturbed to evaluate the tracking capability of the method. Fig. 4 shows the power spectral density (PSD) of a sample signal before and after interference cancellation. As can be seen in Fig. 4(c), all the harmonics are significantly attenuated. To illustrate the drawback of using notch filters, the result of notch filtering at 60 Hz and its multiples is also presented. As shown in Fig. 4(d), the notch filters failed to completely suppress the harmonics because the actual fundamental frequency was not exactly fixed at 60 Hz. Moreover, the notch filters have severely distorted the signal at frequencies around 60 Hz and its harmonics. Fig. 4(e) illustrates the fast convergence of the algorithm where the estimated components (frequency, amplitude, phase) reach the steady state within 200 ms.

In addition to the PSD results shown in Fig. 4, quantitative analysis have been carried out to evaluate the performance

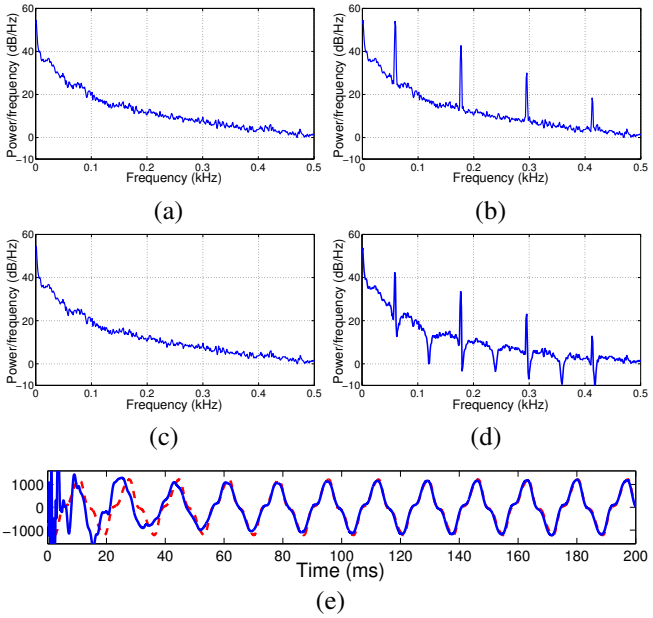

Fig. 4. Simulation results. (a) PSD of the interference-free recordings used in the simulation. (b) PSD after adding synthesized interference. (c) PSD after using the proposed method. Note that all the harmonics are removed while the signal retained (d) PSD after using conventional notch filter. (e) The synthesized (dashed red) and the estimated interference (solid blue).

of interference rejection. Signal-to-interference-ratio (SIR) is defined as the power of the original signal to the power of the synthesized interference. For the heavily contaminated samples (SIR<0 dB), the achieved SIR improvement was as high as 60 dB; while for the samples with small power line interference (SIR>30 dB), the SIR improvement remained positive, implying that the algorithm works reliably and adds very small distortion to LFP signals.

B. Evaluation on Real Data

The second experiment has been carried out on in-vivo data which were recorded by a Plexon system. Fig. 5 shows the PSD of the signal before and after filtering. Large interference components can be seen in Fig. 5(a) at around 60 Hz and its harmonics. It can be seen from Fig. 5(b) that the interference has been completely removed from the contaminated signal. A segment of actual and filtered signal in the Gamma band ($>$ 30 Hz) is also shown in Fig. 5(c).

V. Conclusion

A robust and efficient power line interference cancellation algorithm has been proposed. The proposed algorithm can reject 50/60 Hz noise and its harmonics without producing major distortion to the LFP signals. Moreover, the proposed method can reliably track the fluctuations in frequency, phase and amplitude of interference harmonics. In addition, the low computational cost and small memory requirement of the algorithm has made it suitable for real-time applications. The algorithm is tested on both synthesized and in-vivo data. The results from the synthesized data have shown significant improvement of SIR. In the experiments with the in-vivo

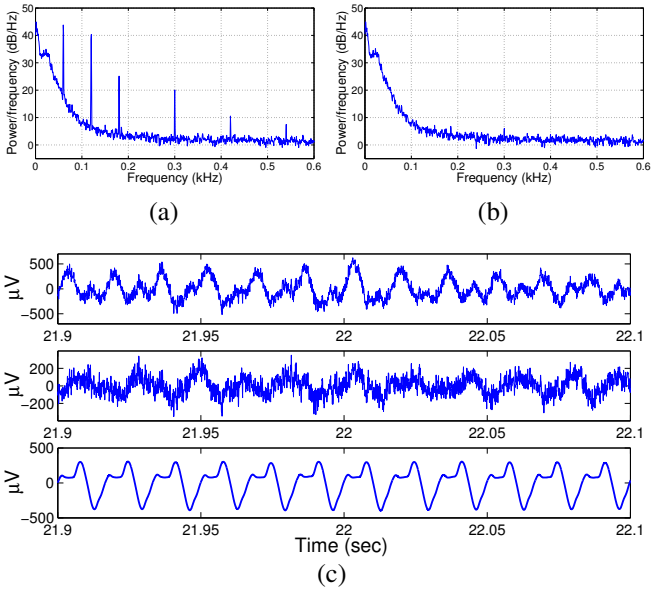

Fig. 5. Results of the experiment with real data. (a) PSD of the contaminated signal. (b) PSD after filtering by the proposed method where the LFP oscillations retained. (c) Gamma band ($>$ 30 Hz) oscillations, from top to bottom: contaminated signal, signal after interference cancellation, estimated interference.

data, the interference has been largely attenuated while the LFP signals have been preserved.

Acknowledgement

The authors would like to thank P. A. Regalia for his help in implementing the ANF [9], and Edward Keefer at Plexon and Victor Pikov at HMRI for providing experimental data.

References

[1] M. A. Lebedev and M. A. Nicolelis, "Brainmachine interfaces: past, present and future," *Trends in Neurosciences*, vol. 29, no. 9, pp. 536–546, Sep. 2006.

[2] Z. Wang and A. W. Roe, "Trial-to-trial noise cancellation of cortical field potentials in awake macaques by autoregression model with exogenous input (ARX)," *Journal of Neuroscience Methods*, vol. 194, no. 2, pp. 266–273, Jan. 2011.

[3] B. Widrow, J. R. Glover, J. M. McCool, J. Kaunitz, C. S. Williams, R. H. Hearn, J. R. Zeidler, J. Eugene Dong, and R. C. Goodlin, "Adaptive noise cancelling: Principles and applications," *Proceedings of the IEEE*, vol. 63, no. 12, pp. 1692– 1716, Dec. 1975.

[4] S. M. Martens, M. Mischi, S. G. Oei, and J. W. Bergmans, "An improved adaptive power line interference canceller for electrocardiography," *IEEE Transactions on Biomedical Engineering*, vol. 53, no. 11, pp. 2220–2231, Nov. 2006.

[5] M. Ferdjallah and R. E. Barr, "Adaptive digital notch filter design on the unit circle for the removal of powerline noise from biomedical signals," *IEEE Transactions on Biomedical Engineering*, vol. 41, no. 6, pp. 529–536, Jun. 1994.

[6] A. K. Ziarani and A. Konrad, "A nonlinear adaptive method of elimination of power line interference in ECG signals," *IEEE Transactions on Biomedical Engineering*, vol. 49, no. 6, pp. 540–547, Jun. 2002.

[7] B. Widrow and S. D. Stearns, *Adaptive signal processing.* Englewood Cliffs, N.J.: Prentice-Hall, 1985.

[8] N. I. Cho, C. Choi, and S. U. Lee, "Adaptive line enhancement by using an IIR lattice notch filter," *IEEE Transactions on Acoustics, Speech and Signal Processing*, vol. 37, no. 4, pp. 585–589, Apr. 1989.

[9] P. A. Regalia, "An improved lattice-based adaptive IIR notch filter," *IEEE Transactions on Signal Processing*, vol. 39, no. 9, pp. 2124–2128, Sep. 1991.

[10] C. Turner, "Recursive discrete-time sinusoidal oscillators," *Signal Processing Magazine, IEEE*, vol. 20, no. 3, p. 103111, 2003.